

# Active Damping Control System in Structures for Seismic Risk Mitigation

**Churong Chen, Cheng-Hsuan Hsu, Sebin Oh, Kurt Soncco, Qinhan Zhou**

*University of California, Berkeley*

May 5th, 2024

## Abstract

Structures are subjected to many different hazards in human history, among which earthquakes are one of the most destructive and common ones. Since 1900, earthquakes have resulted in the deaths of approximately 8.5 million people and have caused damage amounting to 2 trillion dollars. Adding seismic protective systems is a common and popular strategy to mitigate seismic response. The active control system, compared to the passive and semi-active ones, is more flexible, versatile, and effective in serving under different ground motions due to this key feature of providing damping force using external power such as electricity. The main problem in terms of using active control systems to mitigate seismic response is that they heavily rely on external power and the battery can be easily out of power if not being used in a cost-effective way. Our mission in this project is to design the control process using the reinforcement learning method, making sure that the devices will control the seismic response in an acceptable manner while using the minimum external power. The introduction section will demonstrate the background of the earthquake protective systems and the focus will be on the active control ones. Then a literature review will be conducted to summarize how the researchers designed the active control parts and what methods they used to make the real-time decision in recent years. The problem statement and methodology part will demonstrate our problem setups in detail and explain our methodology, which is reinforcement learning, within the scope of our problem. After the previous statements of both the background and methodology, the results of our training model will be shown, and the efficiency of the algorithm will be discussed. Finally, the conclusion part will summarize the whole report and list the key results that we gained.

## 1. Introduction

Protecting the structures in seismic active zones is a major mission for structural engineers since the damage and casualty the earthquakes cause are unacceptable for our society. Those seismic protective systems' main goals and functions are to mitigate the seismic response of the structures and to attenuate the vibration transmitted to the superstructures.

Seismic control systems are commonly divided into three categories, which are passive control systems, semi-active control systems, and active control systems. The passive control ones provide a fixed damping ratio to the structures to attenuate the vibrations and the damping force depends only on the structure response at the locations of the dampers. The typical passive control systems include base isolation systems

and tuned mass dampers. Semi-active control systems can be seen as a compromise between the passive ones and the active ones, which maintain the basic features of the passive control systems while utilizing the external power with a relatively small value. Active control systems rely fully on external power, like batteries, to supply the control force to the structures.

The key difference between the active control systems and the passive control systems is that the active ones have sensors, controllers, and actuators that can make real-time decisions on how much force to provide to the structures. In recent years, it has become a heating topic to employ different methods in controlling the systems.

The greatest challenge so far is to estimate the uncertainties in the seismic excitations. The previous work to solve this problem employed different strategies, including robust control, fuzzy logic control (FLC), and fuzzy gain scheduling.

Our project employs a reinforcement learning method to control the damping ratio in real time based on the structural response while minimizing the power of the process costs.

## 2. Literature Review

The literature review for this project emphasizes the importance of accurate identification and modeling of nonlinear dynamic systems with hysteresis/inelastic behavior for effective seismic risk mitigation. A relevant study by Lai and Nagarajaiah (2019) proposed a sparse structural system identification method that utilizes sparse regularization for parametric modeling. This technique can discern the underlying governing equations of nonlinear systems from input-output data, enhancing the ability to identify significant nonlinearities and hysteresis.

Further literature indicates that current approaches to system identification in structural engineering can be divided into parametric and non-parametric methods. Parametric methods often involve predefined models whose parameters are updated based on measurement data. In contrast, non-parametric methods, such as statistical learning and sparse regression, rely solely on input-output data mapping. They can reveal embedded patterns in the data but may need more straightforward physical insight into nonlinear dynamics.

The study by Lai and Nagarajaiah expands on the work of Brunton et al. (2016), adding functions that capture significant hysteresis and inelastic behavior. Their framework is versatile and capable of identifying different types of nonlinearities and handling data from real-world structures. The effectiveness of the method was validated through numerical simulations and experimental data, highlighting its potential to identify governing equations and parameters that characterize dynamic behavior in a range of nonlinear structural systems.

In another literature review, Akira Saito and Tomohiro Kuno (2020) provide significant insights into experimental modal analysis using Dynamic Mode Decomposition (DMD). Their research explores DMD's capability to accurately identify and extract modal parameters of linear mechanical systems, a process essential for seismic hazard mitigation. They compare the performance of DMD against traditional methods like the Ibrahim Time Domain (ITD) and the Least Squares Complex Frequency (LSCF) method.

Saito and Kuno apply DMD to various systems, including single and multi-degree-of-freedom systems, and evaluate its robustness against measurement errors. The study emphasizes the importance of singular value rejection to remove noise from data, particularly when DMD is used on large-scale data such as

image-based measurements. The results indicate that DMD, coupled with singular value rejection, accurately identifies natural frequencies and mode shapes. However, damping ratios remain challenging to capture accurately due to noise in experimental data.

The authors also experimentally validated their method using data from an impulse response of a cantilever beam. They find that DMD, with proper noise handling, identifies modal parameters comparable to those obtained using the LSCF method and finite element models. This research demonstrates that DMD has potential for modal analysis, particularly when dealing with large datasets. However, more work is needed to improve the accuracy of damping ratio estimates in the presence of noise.

Active control systems play a crucial role in mitigating undesirable vibrations or movements within a structure. By exerting forces that counteract the direction of motion, these systems effectively diminish the energy within the system, contributing to its stability and overall performance. In the literature review, Life Cycle Cost Analysis (LCCA) in the optimization process provides the economic aspects of damping ratio optimization on semi-active and passive systems, considering factors such as repair costs and the initial construction (Aghajani, 2023). The research indicates that an initial increase in damper cost can lead to a reduction in expected total damage costs. By integrating these insights into our report, we aim to provide a holistic approach to structural optimization, emphasizing the interaction between engineering performance and economic considerations. This approach ensures that the damping strategy not only enhances structural resilience but also offers cost-effective solutions.

### **3. Problem Statement and Methodology**

#### ***3.1. Overall problem statement***

Active control systems hold great promise for improving structural safety in earthquake-prone areas due to their ability to adapt damping forces dynamically. Unlike passive and semi-active systems, active control systems leverage external power sources, such as electricity, to provide damping force and adapt to varying seismic excitations. This flexibility, however, brings a significant challenge: active systems are heavily reliant on their external power source, and prolonged or ineffective usage can quickly drain the system's power supply. This makes cost-effective power management a critical concern when aiming to maximize both system effectiveness and longevity.

The central problem that this project addresses is designing an intelligent control process that enables active control systems to deliver optimal damping forces while conserving power usage. This requires a system capable of real-time decision-making to adjust the damping ratio effectively in response to varying seismic inputs, ensuring structures are protected while minimizing the external power draw. Current methods like robust control and fuzzy logic control have been explored, but further improvement in precision and adaptability is needed.

To meet this challenge, our project utilizes reinforcement learning to develop a control system that dynamically adjusts damping forces based on the seismic response of the structure, with the goal of conserving power usage. By training models on real-world data, we aim to create an intelligent system that can predict and apply the optimal damping forces, allowing structures to withstand seismic forces with minimal power consumption. This approach will address the key challenges of cost-effective power usage

and real-time adaptability in active control systems, potentially setting a new standard for seismic protection technology.

### 3.2. Structural modeling using Bouc-Wen model

The modeling approach based on an idealized single degree of freedom (SDOF) system is widely used to simulate structural responses under earthquake ground motions. In such an approach, a structural system is simplified in terms of a global degree of freedom or modeled as an assembly of SDOF systems representing interconnected elements. The following second-order nonhomogeneous ordinary differential equation describes such an idealized SDOF system subjected to ground motions:

$$m\ddot{u} + c\dot{u} + f_s(u, \dot{u}) = -m\ddot{u}_g(t) \quad (1)$$

where  $u$ ,  $\dot{u}$ , and  $\ddot{u}$  respectively denote the relative displacement, velocity, and acceleration of the system;  $m$  is the mass;  $c$  is the damping ratio;  $\ddot{u}_g(t)$  is the time-dependent ground motion; and  $f_s$  is the resisting force describing the force-displacement relationship. The Bouc-Wen model describes the hysteresis behavior of a structural element by introducing a hysteretic displacement  $z$  to the resisting force in Eq. (1) in the form

$$f_s(u, z) = \alpha k_0 u + (1 - \alpha) k_0 z \quad (2)$$

where  $\alpha$  is the post-to-preyield stiffness ratio; and  $k_0$  is the initial stiffness. Among various Bouc-Wen class models, a Bouc-Wen-Baber-Noori (BWBN) model is widely used to represent the hysteretic behavior of reinforced concrete structures and is adopted in this project as well. The hysteretic displacement  $z$  in the BWBN model follows a nonlinear differential equation

$$\dot{z} = \frac{h(z, \varepsilon)}{\eta(\varepsilon)} \dot{x} (1 - |z|^n (\beta \text{sgn}(\dot{x}z) + \gamma) v(\varepsilon)) \quad (3)$$

where  $h(z, \varepsilon)$ ,  $\eta(\varepsilon)$ , and  $v(\varepsilon)$  are the functions of the cumulative energy  $\varepsilon$ , introduced to describe the pinching effect and degradations in stiffness and strength, respectively;  $\beta$  and  $\gamma$  are the basic shape parameters describing the hardening and softening of the material, respectively; and  $\text{sgn}(\cdot)$  is the signum function. The cumulative dissipated energy  $\varepsilon$  is defined by the rate equation as follows:

$$\dot{\varepsilon} = (1 - \alpha) k_0 z \dot{u}. \quad (4)$$

The detailed mathematical expressions for  $h(z, \varepsilon)$ ,  $\eta(\varepsilon)$ , and  $v(\varepsilon)$  are not the focus of this project and thus are omitted for brevity.

### 3.3. Problem formulation as a Markov Decision Process

The Markov Decision Process (MDP) for this problem is defined as follows. The underlying assumption is that the damping of a structure is updated (controlled) every 0.5 second, not every time step (0.02 second for typical earthquake ground motion data). This is to make our problem setting more realistic and to enhance the training performance of the Deep Q-learning by providing more input information. The details of states, transitions between states, actions, rewards, and the discount factor are provided below:

- **States:** The state of the environment at the  $t$ -th time duration,  $\mathcal{S}_t$ , includes the displacement history  $\mathbf{u}_t$  and the cumulative dissipated energy history  $\boldsymbol{\varepsilon}_t$  for the  $t$ -th time duration, and the damping ratio  $c_t$  during the  $t$ -th time duration. Since we assumed that the agent operates the control system every 0.5 second and the time step for typical ground motion data is given as 0.02 second,  $\mathbf{u}_t$  and  $\boldsymbol{\varepsilon}_t$  are

the vectors of length 25. The damping ratio is not updated during each time duration, and  $c_t$  is given as a scalar value. Although  $c_t$  is a single element, a vector of length 25 with repeated  $c_t$  values is used to match the dimensions of  $\mathbf{u}_t$  and  $\boldsymbol{\varepsilon}_t$ . Finally, the state of the environment at the  $t$ -th time duration,  $\mathcal{S}_t$ , is a matrix of dimension 3 by 25.

- **Actions:** The action of the agent at  $t$ -th time duration,  $\mathcal{A}_t$ , can be defined as  $\mathcal{A}_t = [-1 \ 0 \ 1]^T$  where  $-1$  and  $1$  represent the action of decreasing and increasing the damping ratio  $c_t$  by  $0.01$ , i.e.,  $c_{t+1} = c_t \pm 0.01$ , respectively, and  $0$  denotes the actions of keeping the damping ratio to the current value, i.e.,  $c_{t+1} = c_t$ .
- **Transitions:** Given  $\mathcal{S}_t$  and  $\mathcal{A}_t$ , the state of the environment at the  $(t + 1)$ -th time duration,  $\mathcal{S}_{t+1}$ , is determined as  $\mathcal{S}_{t+1} = \mathbf{g}(\mathcal{S}_t, \mathcal{A}_t, \mathbf{g}m_t)$  where  $\mathbf{g}(\cdot)$  represents the nonlinear dynamic analysis of the target structure under the given ground motion  $\mathbf{g}m_t$  for the  $t$ -th time duration. The Bouc-Wen model is used to implement this nonlinear dynamic analysis, which is detailed in Appendix.
- **Rewards:** The reward function  $\mathcal{R}_t$  is composed of two factors: (1) the amount of risk reduction in terms of collapse by choosing the action and (2) the cost of operating the control system. The second term is introduced because otherwise the optimal policy is obvious; always take the action of increasing the damping ratio that reduces the risk of a structure collapsing. The risk for state  $\mathcal{S}_t$ ,  $RISK(\mathcal{S}_t)$ , is defined as

$$RISK(\mathcal{S}_t) = \begin{cases} M_0 & \text{if } \max(\mathbf{u}_t) \geq u_{thres} \text{ or } \max(\boldsymbol{\varepsilon}_t) \geq \varepsilon_{thres} \\ M_0 w \left( \frac{\max(\mathbf{u}_t)}{u_{thres}} \right)^2 + M_0 (1 - w) \left( \frac{\max(\boldsymbol{\varepsilon}_t)}{\varepsilon_{thres}} \right)^2 & \text{else} \end{cases}$$

where  $w$  controls the weights between the effects of displacement and cumulative dissipated energy in the collapse,  $M_0$  denotes a big number corresponding to the collapse event,  $u_{thres}$  and  $\varepsilon_{thres}$  represent the threshold values for the displacement and the cumulative dissipated energy. The cost function is defined as the function of the damping ratio and the action as follows:

$$COST(c_t, \mathcal{A}_t) = \begin{cases} 0 & \text{if } \mathcal{A}_t = -1 \\ cost_{mt} \cdot |c_t - c_0| & \text{if } \mathcal{A}_t = 0 \\ cost_{ct} + cost_{mt} \cdot |c_t - c_0| & \text{if } \mathcal{A}_t = 1 \end{cases}$$

Finally, the reward function  $\mathcal{R}_t$  is defined as

$$\mathcal{R}_t(\mathcal{S}_t, \mathcal{A}_t, \mathcal{S}_{t+1}) = -(RISK(\mathcal{S}_{t+1}) - RISK(\mathcal{S}_t)) - COST(c_t, \mathcal{A}_t).$$

In this project,  $M_0 = 100,000$ ,  $w = 0.5$ ,  $u_{thres} = 9$  mm,  $\varepsilon_{thres} = 13$  kN·mm,  $cost_{mt} = 15$ ,  $cost_{ct} = 0.1$ , and  $c_0 = 0.05$  are used.

- **Discount factor:** The discount factor  $\gamma$  is assumed to be 1.0.

### 3.4. Solution Method: Deep Q-Networks

We chose the Deep Q-Networks (DQN) to solve our MDP problem for the following reasons. First, the dimension of the state variable for our problem is 3 by 25, which is high-dimensional. It is well known that the DQN is particularly effective when dealing with environments where the state space is high-dimensional (Sutton & Barto, 2018). Next, unlike the traditional Q-learning that requires discretizing the state space, DQN can handle continuous state space directly. Last, the reward function for our problem is complex, which leads the decision-making process for the agent to be highly nonlinear and complex. For these reasons, the DQN is adopted as a solution for our problem.

The architecture of the DQN used in this project is illustrated in Figure 1, which consists of two hidden layers, each involving 32 and 8 nodes, respectively, and has the Relu function as an activation function. The output layer has 3 nodes to obtain the Q-values for each of three actions.

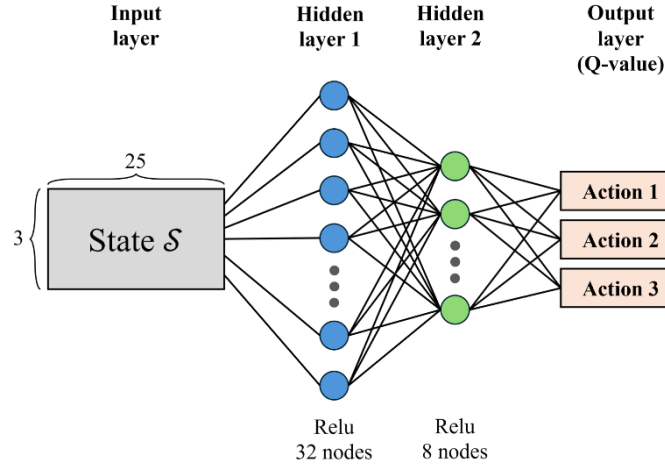


**Figure 1. Architecture of the DQN used in this project**

The overall structure of this project's problem as a reinforcement learning problem is illustrated in Figure 2.

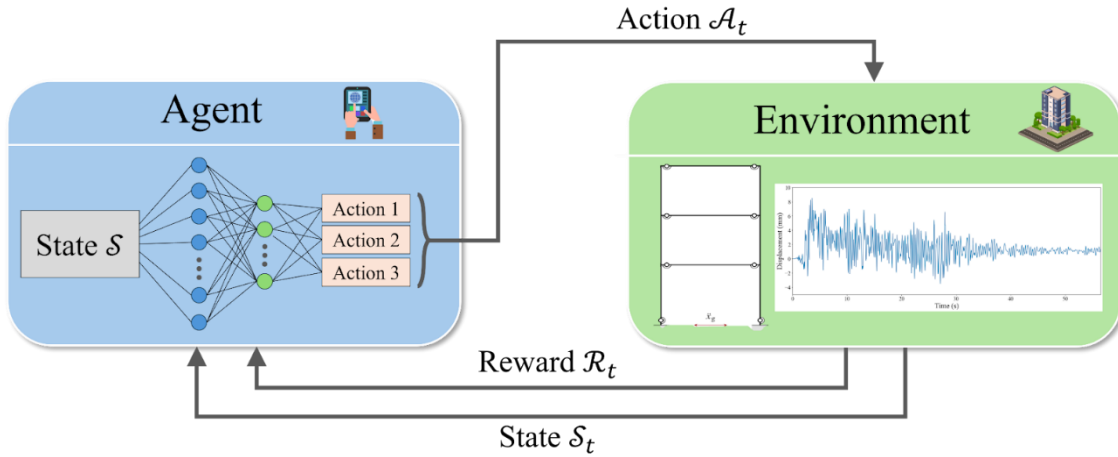


**Figure 2. Overall structure of the control problem of this project as a reinforcement learning problem**

## 4. Results

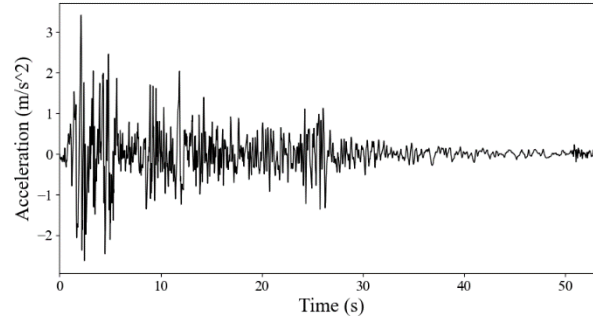
### 4.1. Target structure

To make a numerical example realistic, the parameters of the Bouc-Wen model are estimated from the real experimental data for a reinforced concrete column, which is provided in the Structural Performance Database compiled by the Pacific Earthquake Engineering Research (PEER) center (Berry et al., 2004). The estimated Bouc-Wen model parameters along with the mass and initial damping ratio for the reinforced concrete column are given in Table 1.

**Table 1. Structural properties and Bouc-Wen model parameters for the target structure**

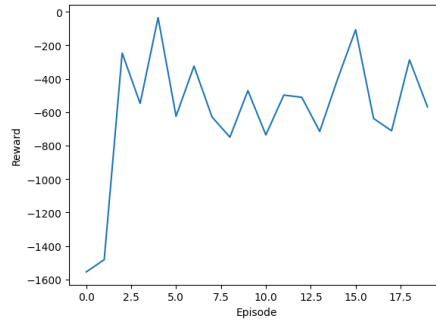
No.	Parameter	Description	Estimated value
1	$m$	Mass (kg)	5000 kg
2	$c$	(Uncontrolled) Damping ratio	0.05
3	$k_0$	Initial stiffness	7.44 kN/mm
4	$F_y$	Yield force	17.42 kN
5	$\alpha$	Post-yield stiffness ratio	0.0138
6	$\beta(= 1 - \gamma)$	Basic hysteresis shape control	0.8897
7	$n$	Sharpness of yield	1.8038
8	$\delta_v$	Strength degradation ratio	0.0002
9	$\delta_\eta$	Stiffness degradation ratio	0.0015
10	$\zeta_0$	Measure of total slip	0.8025
11	$p$	Pinching slop	0.1965
12	$q$	Pinching initiation	0.0137
13	$\psi$	Pinching magnitude	0.8539
14	$\delta_\psi$	Pinching rate	0.0046
15	$\lambda$	Pinching severity	0.1919

For the earthquake ground motion, the historical ground motion data for the 1940 El Centro earthquake was used, which is illustrated in Figure 3.

**Figure 3. Ground motion for the 1940 El Centro earthquake**

#### 4.2. DQN training results

The DQN in Figure 1 was trained for the target structure of Table 1 over 20 episodes. The  $\epsilon$ -greedy policy was adopted with  $\epsilon = 0.1$ , and the learning rate of 0.1 was used. Figure 4 illustrates the DQN training results.

**Figure 4. DQN training results**

### 4.3. Control over the ground motion used in DQN training

Using the trained DQN, the target structure under the 1940 El Centro earthquake is controlled to reduce the seismic risk. Figure 5 compares the displacement history of the original and the controlled systems under the earthquake ground motion with the displacement threshold value marked in red, which demonstrates the efficacy of the agent in terms of reducing the maximum displacement that is crucial in determining the collapse of a structure. Figure 6 compares the cumulative dissipated energy history of the original and the controlled systems, and it also shows that the controlled system remains safe during the whole earthquake while the original system is about to reach the threshold value. Furthermore, it is noteworthy that, in Figure 7 that shows the history of the damping ratio, the damping ratio of the structure returns to the initial damping ratio (inherent damping ratio of the target structure) after strong ground motions have been passed. This balanced control would be beneficial not only for the seismic risk mitigation, but also for the efficient and sustainable operation of the control system.

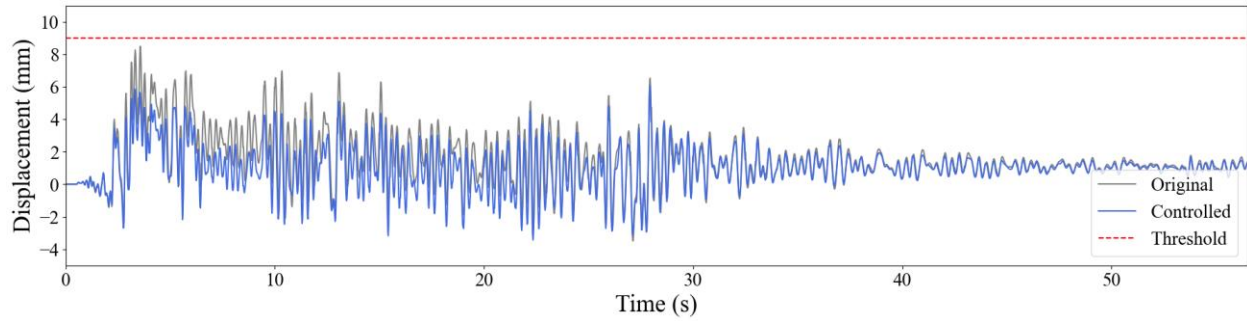


**Figure 5. Comparison between the displacement history of the original and controlled systems under the El Centro earthquake. The red dotted line denotes the threshold value for the displacement (9mm).**

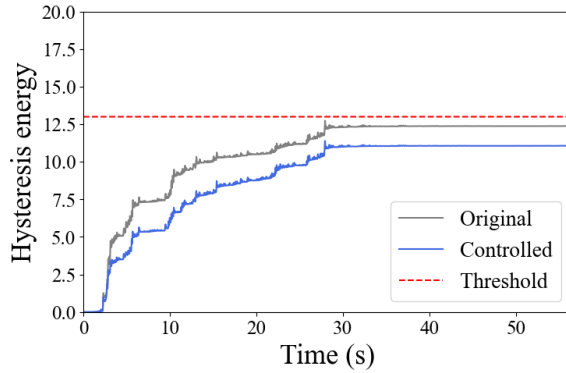


**Figure 6. Comparison between the cumulative energy history of the original and controlled systems under the El Centro earthquake. The red dotted line denotes the threshold value for the cumulative energy (13 kN·mm).**

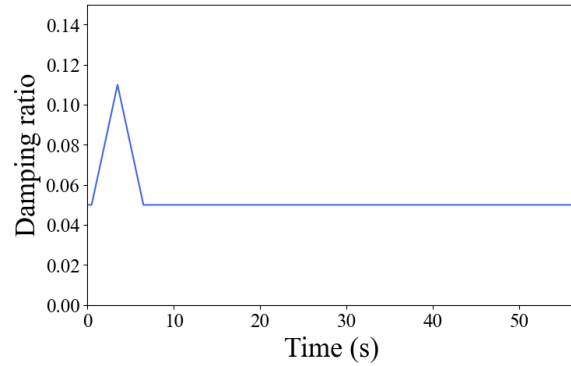


**Figure 7. The history of damping ratio of the target structure under control**



#### 4.4. Control over ground motions for another earthquake

To check if the agent works well for other earthquakes other than the El Centro earthquake that was used to train the DQN, we applied the trained DQN to another empirical ground motion data for the 1989 Loma Prieta earthquake. Figure 8 shows the ground motion history for the earthquake.

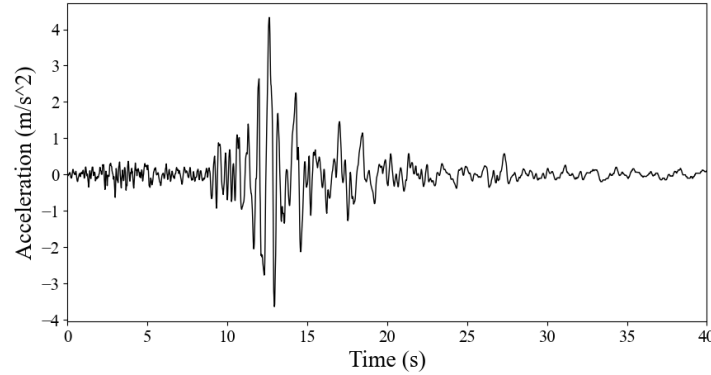


**Figure 8. Ground motion for the 1989 Loma Prieta earthquake**

Figures 5 to 7 illustrate the control results for the target structure under the 1989 Loma Prieta earthquake. Like the El Centro earthquake, the controlled system becomes much safer in terms of the maximum displacement and the final cumulative energy value compared to the uncontrolled system. However, unlike the case of the El Centro earthquake, in Figure 11, the damping ratio increases up to 0.5, which is the maximum damping ratio value that has been set in the code. It means that the agent fails to return the damping ratio value to the initial damping ratio so that we can operate the control system economically. The possible reason for this problem includes that the cumulative dissipated energy has already exceeded the threshold value (see Figure 10) so the reward function does not work properly. Another possibility lies in the different characteristics observed in the displacement histories. The overall shapes of the displacement history are different for the El Centro earthquake and the Loma Prieta earthquake in the sense that the El Centro earthquake induces clearly asymmetrical displacement history while the target structure showed quite symmetrical displacement history for the Loma Prieta earthquake. Considering that the DQN was trained over the El Centro earthquake, the different features observed in the response history might affect the control performance of the agent.

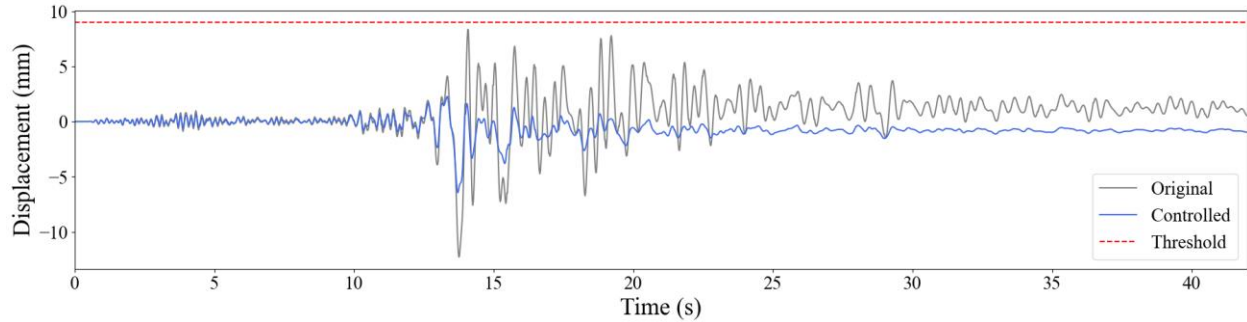


**Figure 9. Comparison between the displacement history of the original and controlled systems under the Loma Prieta earthquake. The red dotted line denotes the threshold value for the displacement (9mm).**

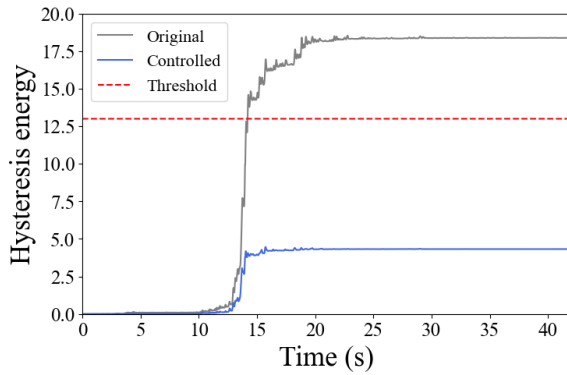


**Figure 10. Comparison between the cumulative energy history of the original and controlled systems under the Loma Prieta earthquake** The red dotted line denotes the threshold value for the cumulative energy (13 kN·mm).

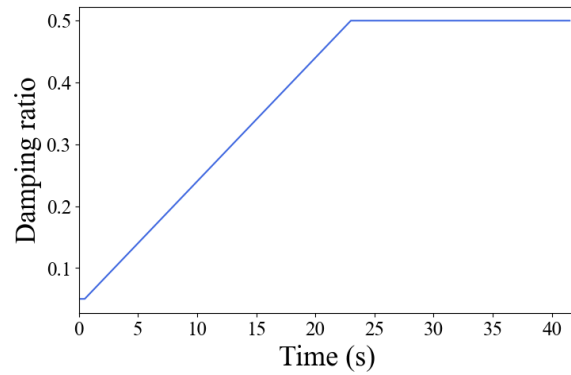


**Figure 11. The history of damping ratio of the target structure under control**

## 5. Conclusions

In this project, we have applied the reinforcement learning to a structural system to mitigate the seismic risk while minimizing the operational cost for the control system. Considering that damping is typically the most critical factor related to the seismic performance of a structure, and at the same time, the most straightforward factor to be controlled, we focused on the control of the damping ratio of a structure. One of the most widely used models for reinforced concrete structures, Bouc-Wen model, is adopted to simulate the dynamic responses of a reinforced concrete structure. Based on the thorough formulation of the problem in the framework of a Markov Decision Process, the Deep Q-Network is adopted to solve the problem due to the high dimensionality, continuity of the state space, and complicated decision process.

Realistic numerical example was performed by estimating the Bouc-Wen model parameters from the real experimental dataset for a reinforced concrete column and by using the empirical ground motion of the historical earthquakes. The DQN was trained with appropriately set hyperparameters over 20 episodes where each episode involves more than 100 training processes. The comparison between the original (uncontrolled) system and the controlled system revealed that the control system significantly reduced the risk not only from the earthquake that was used in training procedure but also from another earthquake, demonstrating the effectiveness and efficacy of the proposed control system.

In this project, however, it was observed that the training process was not stable, and we were not able to train the DQN more than 100 episodes where the DQN consistently returns the actions of staying regardless of the current state. This issue is mainly due to the definition of the reward function and the uncertain nature of earthquakes. The performance of the control system is highly dependent on how the reward function is defined, and the definition of the reward function can reflect which factor (risk mitigation and economics) the decision maker values more. The highly nonlinear and uncertain nature of earthquakes may also affect the training performance of the DQN in the sense that the DQN cannot distinguish whether the increase in risk is due to the inappropriate action or to the ground motion.

## Reference

- [1] Lai, Z., & Nagarajaiah, S. (2019). Sparse structural system identification method for nonlinear dynamic systems with hysteresis/inelastic behavior. *Mechanical Systems and Signal Processing*, 117, 813-842.
- [2] Saito, A., & Kuno, T. (2020). Data-driven experimental modal analysis by dynamic mode decomposition. *Journal of Sound and Vibration*, 481, 115434.
- [3] Sutton, R. S., & Barto, A. G. (2018). *Reinforcement learning: An introduction*. MIT press.
- [4] Aghajani, M., & Asadi, P. (2023). Life-cycle cost analysis of steel frames with shape-memory alloy based dampers. *Structures*, 52, 794-812.
- [5] Berry, M., Parrish, M., & Eberhard, M. (2004). PEER structural performance database user's manual (version 1.0). University of California, Berkeley.

## Appendix: Dynamic analysis of an SDOF system using the Bouc-Wen model

The nonlinear dynamic time history analysis of a structure can be performed using the Bouc-Wen model with the appropriate substitution of the structure to an SDOF system. This dynamic analysis requires a numerical integration scheme, and in this project, the Runge-Kutta method is used. Since the Runge-Kutta method requires the equation of motion to be converted into a system of first-order ordinary differential equations, the equation of motion for an SDOF system for the structure of interest in Eq. (1) is transformed into a first-order, state-space equation of the form as

$$\dot{\mathbf{y}} = \mathbf{g}(\mathbf{y}) + \mathbf{f} \quad (\text{A1})$$

where  $\mathbf{y} = [u \quad \dot{u} \quad z \quad \varepsilon]^T$ ,  $\mathbf{f} = [0 \quad -\ddot{u}_g(t) \quad 0 \quad 0]^T$ , and

$$\mathbf{g}(\mathbf{y}) = \begin{bmatrix} \dot{u} \\ -(c\dot{u} + \alpha k_0 u + (1 - \alpha)F_y z)/m \\ \dot{z}(u, \dot{u}, z, \varepsilon) \\ \dot{\varepsilon}(u, \dot{u}, z) \end{bmatrix}$$

where  $\dot{z}(u, \dot{u}, z, \varepsilon)$  and  $\dot{\varepsilon}(u, \dot{u}, z)$  can be found from Eqs. (3) and (4), respectively. Finally, dynamic analysis for an SDOF system with the Bouc-Wen model can be performed by solving Eq. (A1) using a numerical integration scheme.